Relationships between the Texture and Structure of BaTiO₃ and Its Tetragonal → Cubic Transition Enthalpy

F. J. Gotor, C. Real, M. J. Dianez, and J. M. Criado

Instituto de Ciencias de los Materiales de Sevilla, Apdo. 1115, Sevilla, Spain

A nanometric BaTiO₃ powder sample with a medium crystallite size $D = 157$ Å has been prepared from the thermal decomposition of $BaTiO(C_2O_4) \cdot 4.5H_2O$ by constant rate thermal analysis (CRTA). Rietveld analysis of the XRD pattern shows that this BaTiO₃ sample presents a crystalline cubic structure. The evolution of the texture, the structure, and the ferroelectric → paraelectric enthalphy transition as a function of the annealing temperature of BaTiO₃ has been followed from XRD and DSC experiments. A relationship has been found between the reaction enthalphy of the tetragonal → cubic polymorphic transition and the tetragonality of the sample, as measured from the c/a ratio. Therefore, the calorimetric data can be used for predicting the structure of this material. The Curie temperature seems to independent of the crystallite size D, provided that it is higher than about 400 Å. © 1996 Academic Press, Inc.

INTRODUCTION

Barium titanate is the most widely used material for the production of multilayer ceramic capacitors (1, 2) since the discovery of its extremely high dielectric constant. It is well known that the small particle size of BaTiO₃ starting powders enables better sintering and the development of uniform microstructure throughout the ceramic component (3). On the other hand, it has been reported (4–10) that the dielectric constant and the Curie temperature (associated to the tetragonal → cubic polymorphic transformation of BaTiO₃) strongly depend on the size. This behavior explains that a variety of methods for yielding ultrafine powders have been proposed in literature (3, 11–17) as an alternative to the common industrial method for producing BaTiO₃, i.e., by annealing equimolecular mixtures of barium carbonate and titania in air at temperatures exceeding 1200°C and leading big particle size.

The scope of the present work is to apply the differential scanning calorimetry (DSC) method for both, analyzing the microstructure of BaTiO₃ and determining its Curie temperature. So far, this method had not been previously used for this purpose. This study requires the preparation of a series of ultrafine BaTiO₃ samples with different crys-

talline size and tetragonality. The barium titanly oxalate sample prepared by us in a previous paper (18) has been used as precursor. We reported (18) that this sample was constituted by small single crystals whose structure was determined from Patterson and Fourier synthesis using 3261 unique X-ray single crystal reflections. The results of the structural analysis allow us to assure that the Ba/Ti ratio is exactly one, and therefore, pure and stoichiometric BaTiO₃ would be obtained from the thermal decomposition of the above precursor. This is important if we take into account that Fang *et al.* (19) have shown that the coprecipitation with oxalate of an equimolar mixture of barium and titanium salts would yield a mixture of oxalates rather than a single compound, depending on the experimental conditions.

EXPERIMENTAL

Preparation of the BaTiO₃ Samples

We have utilized the Clabaugh method (20) using $BaCl_2 \cdot 2H_2O$, $TiCl_4$, and $C_2O_4 \cdot 2H_2O$ (Merck pro analysis) as starting materials. We have shown in a previous paper (18, 21) that the above method leads to the single compound $BaTiO(C_2O_4)_2 \cdot 4.5H_2O$ that crystallizes in the monoclinic system with the following lattice parameters: $a = 13.382(2)$ Å; $b = 13.812(2)$ Å; $c = 14.044(2)$ Å, and $\beta = 91.48(1)°$.

The thermal decomposition of the above precursor has been carried out by constant rate thermal analysis (CRTA) described elsewhere (22, 23). This method implies the control of the temperature of the sample in such a way that both decomposition rate and residual pressure of the gases self-generated in the reaction are maintained constant all over the process at a value previously selected by the user. This has been achieved by using a conventional high vacuum system equipped with pirani and penning gauges. Either the pirani or the penning gauges can be interfaced to the power controller of the furnace. Thus, the temperature of the sample can be monitored in such a way that the pressure of the gases produced in the reaction is main-

tained constant at any value selected by the user in the range from 10^{-6} to 10 mbar. The constant reaction rate can be selected by choosing the proper pumping rate thanks to a butterfly vacuum valve. We must bear in mind that the production rate of gases and, therefore, the decomposition rate of the precursor must be necessarily constant along the whole reaction, providing that both pumping rate and residual pressure are maintained constant.

Methods

The DSC experiments were carried out with a Seteram DSC 111 equipment with a sensitivity of 1 mV/s. A flow of helium of 20 cc/min and heating rate of 3 K/min were used.

Surface area measurements of $BaTiO_3$ powders were carried out with an Adsorpmeter Micromeritic, model 2000, using as adsorbate N_2 at the liquid nitrogen temperature.

The powder diffraction diagrams were recorded with a D-500 Siemens powder diffraction system. Pure monochromatic $CuK\alpha_1$ radiation with $\lambda = 1.54059$ Å was used. The alignment of the diffractometer was better than $0.005°$ (2θ). The diffraction pattern was scanned from 20 to $115°$ (2θ) with a step length of $0.004°$ and a fixed counting time of 60 s. A precise determination of peak positions and integrated intensities was carried out using the fitting program available in the PC software package DIFFRACT-AT supplied by Siemens-Socabin as described Bernard *et al.* (24).

The analysis of the symmetry of the (200) family of diffraction peaks has been used for discerning the crystalline structure of $BaTiO_3$ (9). The full-width of the half maximum (FWHM) of (111) diffraction peak has been used for calculating the medium diameter of the coherently diffracting domain according to the Scheerrer equation,

$$D_{hkl} = 57.3 \ k\lambda/\beta \cos \theta.$$

The tetragonality of the sample has been expressed by the value of the c/a ratio. The a and c lattice parameters were determined by processing all the XRD peaks recorded in the range from $20°$ to $90°$ (2θ) by means of the DICVOL 91 computer program (25) assuming a tetragonal symmetry.

RESULTS AND DISCUSSION

It was reported in a previous paper (23) that the conventional synthesis of $BaTiO_3$ from the thermal decomposition of $BaTiO(C_2O_4)_2 \cdot 4.5H_2O$ under air atmosphere requires us to heat this precursor up to $750°C$ in order to complete the reaction. The $BaTiO_3$ obtained under these experimental conditions has a large particle size and shows a tetragonal structure. Thus, the sample yielded in the present work has been obtained by decomposing the above precursor

TABLE 1

Textural Characteristics of the $BaTiO_3$ Sample Obtained from the Thermal Decomposition of $BaTiO(C_2O_4)_2 \cdot 4.5H_2O$ by Means of the CRTA Method

Sample	Crys.structure	S_{BET} (m²/g)	$D^a_{BET}(\mu m)$	$D_{Scheerer}$(Å)
$BaTiO_3$	cubic ($d = 4.0177$ Å)	14.4	0.07	159

a Calculated from specific surface area by assuming a spheric symmetry according to the formula $d = (6/S_{BET} \cdot \rho)$, where ρ is the density of $BaTiO_3$ (6.01 g/cc).

under vacuum using the CRTA method at a constant rate $C = 2.98 \times 10^{-3}$ min^{-1} (i.e., the reaction is over at $1/C$ representing 335 min). The full conversion to $BaTiO_3$ was reached at about $550°C$ under these experimental conditions but the temperature was allowed to increase up to $750°C$ and annealed at this temperature for 1 h under vacuum. Table 1 shows the specific surface area determined for this sample together with the medium particle size $D_{\eta s}$ calculated from the BET surface by assuming spherical symmetry and the size of the coherent diffraction domain D_{111} calculated from the FWHM of the (111) diffraction peak. The large difference between the particle size determined from the BET surface and the coherent diffraction domain size calculated from X-ray diffraction analysis can be explained by assuming that the $BaTiO_3$ particles are not single crystals, as Uchino *et al.* (9) have suggested, but that they are constituted by small crystallites (coherently diffracting domains) welded in a mosaic structure. This explanation agrees with results reported in previous papers that show that the microstrains of $BaTiO_3$ (26) and other ceramic materials (27, 28) are decreasing by increasing the size of the coherently diffracting domains. This finding has been explained by assuming that grain boundary constitutes the main contribution to the microstrains of the
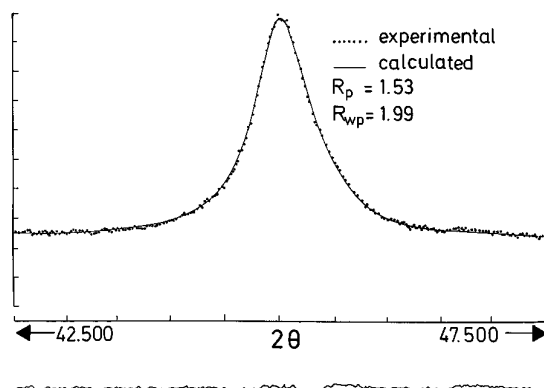

FIG. 1. XRD profile of the $BaTiO_3$ sample described in Table 1 and the final difference plot between the experimental curve and the curve calculated assuming a Pearson VII symmetric function.

TABLE 2
Results Obtained from Rietveld Full Profile Refinement from XRD Data of BaTiO$_3$

a (Å)	4.0177 Å
V	64.85 Å^3
Space group	$Pm\bar{1}3m$
Z	1
Wavelength (Å)	1.54056
2θ range (°)	20–145
$\Delta2\theta$ (°)	0.04
No. of reflections	21
R_p	0.0032
R_{wp}	0.042
R_F	0.032
R_B	0.048

BaTiO$_3$ particles. Therefore, the higher the number of grain boundaries in a particle the lower the size of the crystallites.

Figure 1 shows both the observed (200) XRD profile of the BaTiO$_3$ sample described in Table 1 and the difference between the experimental curve and that calculated by assuming a Pearson VII symmetric function, together with the R_p and R_w fitting parameters. These results point out that the (200) XRD profile is quite symmetric, which means that is not split to peaks. This behavior suggests that the BaTiO$_3$ sample used in this work has crystallized in cubic symmetry.

In order to check the above assumptions both the integrated intensities and the peak positions of the whole XRD diffraction diagram recorded for the BaTiO$_3$ sample described in Table 1 have been fitted by means of the Rietveld refinement program FULLPROF (29). The conditions of the refinement are included in Table 2. The excellent fitting
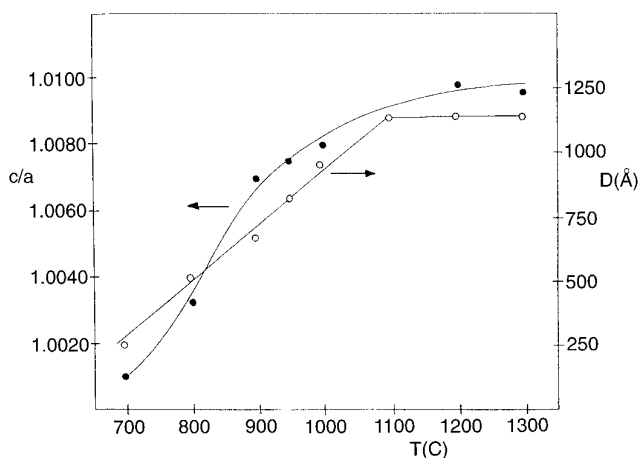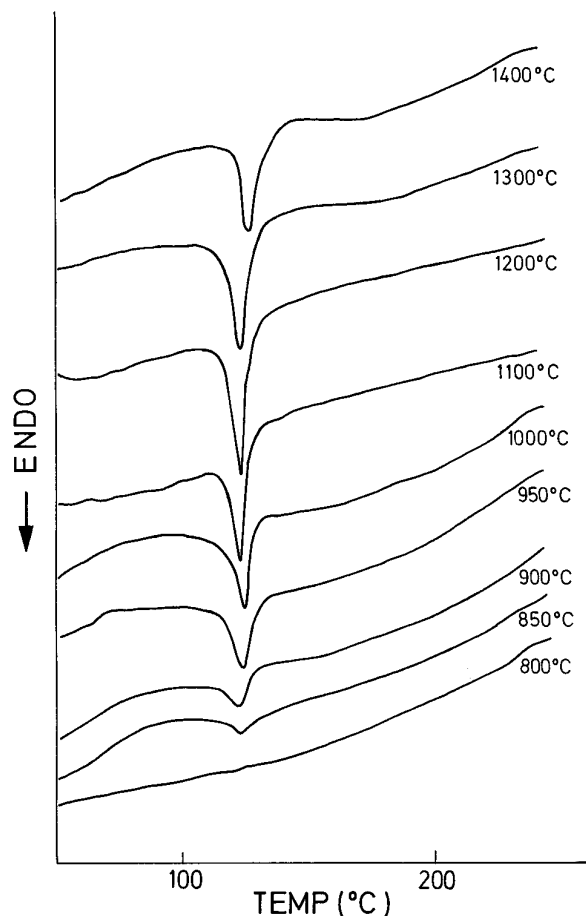

FIG. 3. DSC diagrams for the BaTiO$_3$ sample described in Table 1 after undergoing previous annealing treatment for 1 h at different temperatures.

FIG. 2. Plots of the c/a ratio and the crystallite size as a function of the annealing temperature.

parameters reported here demonstrate that the BaTiO$_3$ sample has a cubic structure.

The evolution of the structure and microstructure of the sample described above has been followed by measuring both tetragonality of the sample and coherent diffraction domain size as a function of the annealing temperature. The tetragonality of the sample has been determined from the full XRD profile analysis as described in the Experimental. The coherently diffracting domain sizes have been calculated from the FWHM of the (111) peak. Figure 2 shows the plot of the c/a ratio and the crystallite size as a function of the annealing temperature. These results point out an increase of the tetragonality of BaTiO$_3$ by increasing its coherently diffracting domain size. Moreover, a c/a value higher than unity is reached at D values around 250–300 Å, which means that values of D lower than 300 Å would be required for stabilizing at room temperature the cubic lattice of BaTiO$_3$. This behavior supports that the stabilization of the cubic phase of BaTiO$_3$ depends on
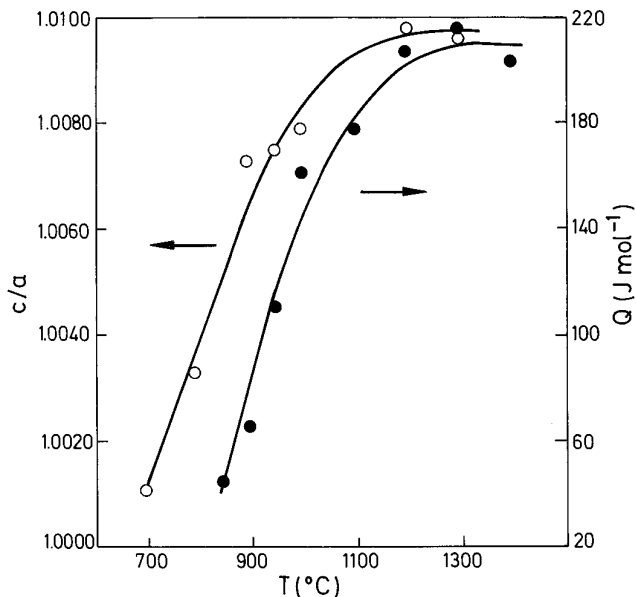
FIG. 4. Influence of firing temperature on both the c/a ratio and enthalpy of the tetragonal $\rightarrow$ cubic transition of $BaTiO_3$.

the coherently diffracting domain size rather than on the particle size as suggested by other authors (4–10).

Figure 3 shows the DSC diagrams recorded for the $BaTiO_3$ sample described in Table 1 after being annealed for 1 h at different temperatures ranging from 800 to 1400°C. The enthalpies of the tetragonal $\rightarrow$ cubic transition of $BaTiO_3$, calculated from the above DSC traces, have been plotted in Fig. 4 together with its respective c/a ratio, as a function of the annealing temperature.

The above results point out that a c/a ratio of about 1.004 is required for observing the endothermic tetragonal $\rightarrow$ cubic phase transition of $BaTiO_3$ on the corresponding DSC diagram. Figure 4 shows that provided that the c/a ratio is higher than the above threshold value, a relationship between the conversion enthalpy and the tetragonality of the $BaTiO_3$ sample can be. Thus, we can conclude that DSC could be a method for estimating the tetragonality of a $BaTiO_3$ sample. Moreover, it has been clearly demonstrated that a relationship exists between coherently diffracting domain size, tetragonality of the sample, and transition enthalpy of the tetragonal $\rightarrow$ cubic conversion of $BaTiO_3$.

On the other hand, it must be pointed out that the peak temperature on the series of DSC diagrams included in Fig. 3 remains constant at 125°C. Thus, the phase transition temperature of $BaTiO_3$ seems to be independent of both tetragonality of the sample and coherently diffracting domain size for a crystallite size longer than about 400 Å. Figure 2 shows that this value is reached after annealing the sample at 850°C. We must keep in mind that the ferro-

electric $\rightarrow$ paralectric transition of $BaTiO_3$ is not recorded on the corresponding DSC diagram unless this sample is annealed at temperatures higher than 850°C, as Fig. 3 shows.

The results previously reported by Uchino *et al.* (9) regarding to the relationship between crystallite size, as determined from broadening of XRD (111) peaks, and the Curie temperature of $BaTiO_3$ are in good agreement with our observations. However, they are in disagreement with the results reported by other authors (6, 7, 10) who have concluded that the Curie temperature increases with increasing particle size in the range from 0.2 to 4 μm. It must be pointed out that these authors have estimated the crystallite size by SEM or TEM and that $BaTiO_3$ particles would be constituted by several crystallites welded in a mosaic structure as we have reported in previous papers (26–28). Thus, we can conclude that the coherently diffracting domain size determined from the broadening of X-ray diffraction peaks is the most appropriate parameter for correlating the crystallite size with the Curie temperature of $BaTiO_3$.

REFERENCES

1. J. F. Fernandez, P. Duran, and G. Moure, *Ferroelectrics* **127,** 65 (1992).
2. G. Goodman, *in* "Ceramic Materials for Electronics, Processing, Properties, and Applications" (R. C. Buchanan, Ed.), pp. 79–138. Decker, New York, 1986.
3. M. Rajendran and M. Subba Rao, *J. Solid State Chem.* **113,** 239 (1994).
4. A. Yamaji, Y. Enomoto, K. Kinoshita, and Murakami, *J. Am. Ceram. Soc.* **60,** 97 (1977).
5. A. J. Bell, A. J. Moulson, and L. E. Cross, *Ferroelectrics* **54,** 147 (1984).
6. G. Artl, D. Hemming, and G. D. With, *J. Appl. Phys.* **58,** 619 (1985).
7. G. Artl, *Ferroelectrics* **104,** 217 (1990).
8. T. Kanata, T. Yoshikawa, and K. Kubota, *Solid State Commun.* **62,** 765 (1987).
9. K. Uchino, E. Sadanaga, and T. Hirose, *J. Am. Ceram. Soc.* **72,** 1555 (1989).
10. R. P. S. M. Lobo, N. D. S. Mohallem, and R. L. Moseira, *J. Am. Ceram. Soc.* **78,** 1343 (1995).
11. S. Kumar and G. L. Messing, *J. Am. Ceram. Soc.* **77,** 2940 (1994).
12. W. E. Rhine, R. B. Hallock, W. Davis, and W. Wong-Ng, *Chem. Mater.* **4,** 1208 (1992).
13. H. J. Schmutzler, M. M. Antony, and K. H. Sandhage, *J. Am. Ceram. Soc.* **77,** 721 (1994).
14. P. K. Dutta, P. K. Gallagher, and J. Twee, *Chem. Mater.* **5,** 1739 (1993).
15. D. Hennings, M. Klee, and R. Waser, *Adv. Mater.* **7**(8), 334 (1991).
16. F. Chaput, J. P. Boilot, and A. Beanger, *J. Am. Ceram. Soc.* **73,** 942 (1990).
17. K. Kajiyoshi, N. Ishizana, and M. Yoshimura, *J. Am. Ceram. Soc.* **74,** 369 (1991).
18. M. Louër, D. Louër, F. J. Gotor, and J. M. Criado, *J. Solid State Chem.* **92,** 565 (1991).
19. T. T. Fang, H. B. Lin, and J. B. Hxxang, *J. Am. Ceram. Soc.* **73,** 3363 (1990).
20. W. S. Clabangh, E. M. Swiggard, and R. Gilchrist, *J. Res. Natl. Bur. Stand.* **56,** 289 (1956).

21. D. Louër, A. Boultif, F. J. Gotor, and J. M. Criado, *Powder Diffr.* **5,** 165 (1990).

22. F. Rouquerol, Y. Laureiro, and J. Rouquerol, *Solid State Ionics* **63–65,** 363 (1992).

23. J. M. Criado, F. J. Gotor, C. Real, F. Jimenez, S. Ramos, and J. del Cerro, *Ferroelectrics* **115,** 43 (1991).

24. P. Bernard, J. P. Auffredic, and D. Louër, *Powder Diff.* **8,** 39 (1993).

25. A. Boultif and D. Louër, *J. Appl. Crystallogr.* **24,** 987 (1991).

26. J. M. Criado, M. J. Dianez, F. J. Gotor, C. Real, F. Jimenez, S. Ramos, and J. del Cerro, "International Symposium on Applications of Ferro-electrics." IEEE catalog number 90CH2800-1, p. 36. 1990.

27. J. M. Criado, F. Gonzalez, M. Gonzalez, and C. Real, *J. Mater. Sci.* **17,** 2056 (1982).

28. J. M. Criado, M. Gonzalez, and C. Real, *J. Mater. Sci. Lett.* **5,** 467 (1986).

29. J. Rodriguez-Carvajal, *in* "Collected Abstracts of Powder Diffraction Meeting, Toolouse, France," p. 127. 1990.